Comparative study on thermal performance of cross-matrix absorber solar collector with series and parallel configurations

M.A.S.M. Tarminzi [a], A.A. Razak [a,*], M.A.A. Azmi [a], A. Fazlizan [b], Z.A.A. Majid [c], K. Sopian [b]

[a] Energy Sustainability Focus Group (ESFG), Faculty of Mechanical and Automotive Engineering Technology, Universiti Malaysia Pahang, Pekan, Pahang, Malaysia
[b] Solar Energy Research Institute, Universiti Kebangsaan Malaysia, 43600, Bangi, Selangor, Malaysia
[c] Kuliyyah of Allied Health Sciences, International Islamic University of Malaysia, Kuantan, Pahang, Malaysia

A R T I C L E I N F O

A B S T R A C T

This paper presents an experimental study comprising two CMA solar collectors with parallel and series arrangements on a forced convection solar drying system. The parallel and series solar collectors were investigated to evaluate the arrangement type's effect on the thermal performance. The experiments were conducted using artificial solar radiation that varies from 300 to 900W/m2 with the air velocity of 0.5–2 m/s. The arrangement's efficiency was evaluated based on the drying chamber's thermal delivery from the collectors, thermal gains, and drying efficiencies, including air velocity effect and pressure drop. Results show that the solar collectors' parallel arrangement leads to higher air temperature inside the drying chamber than the series by 3.87 °C. The thermal efficiency of 33.89% is achieved for the parallel setup than the series of 27.73%. The series arrangement is superior to the parallel in terms of the pressure drop across the solar drying system. Drying efficiency is observed at a higher air velocity of 2 m/s for both arrangements than lower airflow of 0.5 and 1 m/s. Parallel configuration showed promising performance in drying efficiency and low energy usage compared to the series arrangement in which the negative impact of higher pressure-drop was compensated.

1. Introduction

Solar energy, which is the most resourceful renewable energy, is an alternative to replace fossil fuel as fossil fuel demand increases day by day. The increase in energy price resulting from increasing energy shortage will eventually become a crisis, coupled with the long term energy use, which causes pollution [1]. Solar energy technology must be continuously developed to overcome the problem as its source is inexhaustible. The use of solar energy will help reduce emissions of greenhouse gases that contribute to global warming. Efforts that have been done to increase the efficient use of energy and higher growth of renewable energy applications are beneficial to our community [2]. The transitions to renewable energy sources are innovatively developed by considering in both academic and business sectors in order to create a secular economy and targeted industrial pathway [3]. Solar energy is widely used in various activities, especially in the food industry [4], where air and water are heated to dry agricultural and marine products.

Solar radiation comes in its primary source as heat. Different places will receive different rates of solar radiation since the Earth's surface is not flat; different climatic conditions may also affect the solar radiation received at one particular place. For the equatorial region, the solar

radiation incident to the Earth's surface is not consistent due to highly humid and hot climate, which will lead to cloud formation in the atmosphere. Most of the solar radiation will be reflected back to the outer space by the cloud cover, which comprises water vapour, air molecules and dust particles that further cause diffuse radiation. Hence, only a limited amount of solar radiation is received at the surface of the Earth [5].

Solar dryers have long been developed in two directions. First, a low-cost solar drying system which used to be a simple design with low power usage but will cause a short life and low efficiency. Second, a long life and high-efficiency system because of a more complicated design and higher power utilization (Sivakumar & Rajesh K, 2016). Efforts have been made to improve the efficiency of the solar drying system by analyzing the parameters namely the selection of materials for components in the system, loading and pre-treatments, drying temperature achieved in the drying chamber, the fluid velocity and relative humidity [6]. [7] studied on the configuration of double-pass photovoltaic-thermal hybrid solar collector embeddable in an indirect solar dryer system, and they found that the addition of a glass cover, metal plate and double-pass air flow passage have significantly increased the overall efficiency of the hybrid photovoltaic/thermal air collector. Other than that, improvising the collector design by adding fins can help to rise not only thermal performance but also electrical performance significantly [8].

Solar collectors are installed in a drying system to heat the fluid that passes through so that a variation of targeted temperature can be achieved depending upon the industrial purposes with consistent air temperature output. Drying with an optimum temperature can ensure higher product quality since it will not harm the nutritional value of the products like vegetables and fruits. It is recommended to install solar collectors in a drying system since it can help to achieve higher energy savings due to low maintenance cost [9], which is convenient to the industry. In Krasnodar Region (Russia), potential energy-saving in the food industry can be increased by 16%–17% of the total amount of produced thermal energy in that region annually when a solar collector is brought into production [10].

Optimizing the performance and efficiency of the solar collector must be prioritized by improving the design of the absorber and enhancing the absorber surface with the addition of heat loss reduction from the collector [11]. One can use cross-matrix (CMA) design since it offers the possibility to use multiple types of material for the thermal absorber which can give advantages through combining thermo-physical properties of materials to increase the performance of the absorber [12]. [13] studied four different geometries of CMA to evaluate their efficiency and the result obtained by Type 1 was the highest since it had the optimal solar radiation exposure compared to the other three designs. Further innovation had been done by Ref. [14] by utilizing paraffin as thermal energy storage material to the CMA. It was concluded that the highest mass flow rate of 0.01 kg/s passing through the absorber leads to the higher heat gain by the CMA, hence prolonged the cooling down/discharging period as shown by the result, where a case with maximum mass flow rate (0.01 kg/s) consistently contributed to the higher heat gain by the absorber. Heat storage material was also being applied by Ref. [15] where about 11.8% drying chamber efficiency was improved compared to without heat storage material.

Solar air collectors have a lower investment cost than the solar water collectors due to their materials, which are cheaper and easy to fabricate and requiring low maintenance cost [12]. Since the solar air collectors have a lower chance to be exposed to corrosion and abrasion due to water, a more comprehensive range of materials can be used to construct the structure. However, the drying system for solar air collector is more significant in size compared to solar water collector as higher air mass flow is needed to remove heat compared to water-based collector since the specific heat capacity of air is approximately four times lower than water [16]. The design of the solar collector depends on the capital investment and also the temperature required to carry out the drying process. It can be low-cost air flat-plate collectors which suit any application of low temperature up to 100 °C to more complex design such as Fresnel collector or parabolic trough collectors that can produce heated air up to 400 °C [4].

Solar collectors play an important role in determining the performance of a solar drying system. The number of solar collectors in a drying system varies according to the design and heat requirement of the drying process. The collectors can be arranged either in series or parallel configuration depending on the desired temperature level [17]. An experimental study had been done to analyze the efficiency of evacuated tube solar thermal collector, and the result showed that with the use of same input flow rate to the single collector, the parallel configuration achieved higher efficiency of 15% compared to the series configuration [18]. Meanwhile [19], validate optimum numbers of evacuated tubes that can be used in a solar system. The findings help the researchers and engineers who are working in the solar energy field to choose the best number of evacuated tubes together with their arrangement.

Based on the conducted literature review, there are fewer studies signifies the importance of the difference between the performance of parallel and series arrangement of solar air collector. Most of the previous papers focused on studying and improving the overall solar drying systems' performance without emphasizing on the arrangement of collectors in order to achieve desired fluid temperature and flowrates. The primary purpose of this study is to determine the best collector configuration for the solar dryer, and the results will be crucial for the researcher or practitioner to decide which system they should adapt especially in the tropical weather country such as Malaysia, which the solar radiation is maximized at the mid-day. The augmentation of supplied thermal energy at the outlet of the system will improve the load quality and lead to the improvement of the application related to the solar air heating system such as drying application. Therefore, in this paper, the effect of using series and parallel arrangements of two solar collectors with cross-matrix absorbers are investigated. Thermal performance for both arrangements was observed and compared under several operating parameters, including mass flow rate and solar radiation. Finally, both system performances were evaluated based on the drying process of Kaffir leaves in order to determine the most efficient system configuration for the particular drying process.

2. Methodology

2.1. Solar thermal collectors configurations

Designing thermal absorber and coatings selection are crucial steps to ensure the extraction of solar energy effectively [20]. Two
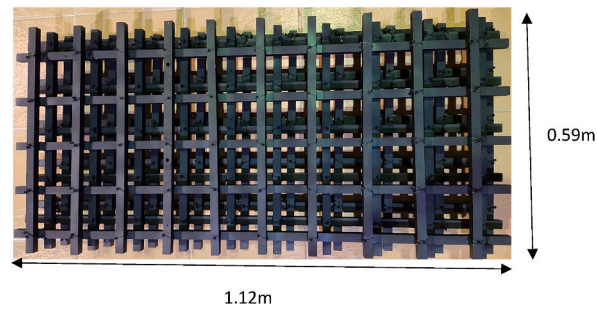
Fig. 1. Measurement for a cross-matrix absorber.

Fig. 2. Solar collectors in series and parallel configurations.

solar collectors with cross-matrix absorbers were fabricated using aluminium square hollow tubes as the material for the structure of the collectors and the absorbers. Each absorber comprises three sets of cross-matrix aluminium to enlarge the solar collection area, as shown in Fig. 1. The absorber was coated with flat black spray to allow maximum heat absorption and to avoid reflected heat to the surrounding (Braendly, 2010).

The primary material for the structure of the solar collector was made of stainless steel. High corrosion resistance and its ability to stand on a high-temperature process make the stainless steel suitable for drying activity. The dimensions for each solar collector was 1.22 m × 0.61 m. The absorber which was made of square hollow aluminium tube with a dimension of 1.17 m length x 0.59 m width x 0.11 m depth was placed inside the collectors and 4-mm thickness of a transparent polycarbonate sheet acting as a top cover component of the collector. It is essential to maximize the absorber size since the potential heat losses are higher when the area for heat transfer is smaller than the area of the project to the absorber [21]. Four air control valves are used to allow the air to flow either in series or parallel mode, as shown in Fig. 2.

An Advantech ADAM® data acquisition system (DAQ) equipped with 52 channels and ADAMView® V4.30 software was utilized throughout the experiment to collect and store data for the assigned parameters, namely temperature, solar radiation intensity and ambient temperature. Each experiment was held for 1 h to observe the temperature changes in the system and the effect of series and parallel arrangements of the solar collector was analyzed.

Choosing the best material for absorber and structure for a collector can result in higher efficiency. Table 1 shows the common materials used to fabricate the absorber. Four materials were compared based on their thermo-physical properties [22]. had done a study on thermal conductivity of absorber plate, and the results showed that copper as thermal absorber has 3% improvement on performance compared to aluminium. Copper has higher thermal conductivity compared to stainless steel, low carbon steel and

Table 1
Thermo-physical properties of absorber material.

Material	Thermo-physical Properties				
	Density: ρ (kg/m^3)	Specific heat: c_p (J/kg K)	Thermal conductivity at 100 °C: λ (W/mK)	Thermal diffusivity at 27 °C: (m/s^2)	Thermal effusivity (Ws$^{1/2}$/m^{2}K)
Stainless steel (304)	8000.0	500.0	16.2	4.2×10^{-6}	22045.4
Aluminium (6063)	2700.0	900.0	200.0	6.4×10^{-5}	8049.8
Copper (1050)	8890.0	385.0	401.0	1.11×10^{-4}	47992.5
Low Carbon Steel (AISI 1010)	7870.0	448	51.9	1.88×10^{-5}	13921.5

aluminium. However, due to the potential of corrosion, copper is not suitable to be used in drying application related to food. Besides, the cost of copper is high and will cause a more extended payback period. Aluminium can be used as an alternative material for solar thermal absorber due to its comparable performance as copper [23] with a lower cost factor. Aluminium is more preferred for the drying process since it is more economical and has acceptable performances.

Even though copper exhibits the highest diffusivity and highest effusivity, which allows it to become susceptible to temperature change, aluminium is more preferred due to its corrosion resistance and low-cost factor. Besides, aluminium generally requires no additional metal treatment and coating to inhibit corrosion as compared to mild steel [16]. Aluminium is convenient in terms of workability. Due to its high strength to weight ratio, aluminium can be easily cut and formed during the fabrication process rather than stainless steel. Besides, aluminium has higher thermal conductivity and has a lower cost factor compared to stainless steel.

2.2. Experimental setup and procedure

A hybrid-active solar dryer, as shown in Fig. 3, was developed in the Laboratory of Engineering Technology, Universiti Malaysia Pahang, Malaysia. The solar dryer consists of several components, namely two solar collectors, a mixing chamber, an auxiliary heater and a drying chamber, as shown in Fig. 3. The system can be operated in three different modes, as presented in Table 2.

Mode 1 was used for the whole experiment for this paper. The experiment was carried out with indoor conditions. Eighteen units of 300W halogens lamps were integrated and used as a solar simulator. The solar simulator was installed with a voltage regulator to control the light intensity. The radiation was measured by using a pyrometer, and the ambient temperature monitored so that it could be controlled with minimal fluctuation. The output measured from the solar simulator ranged from 300 W/m^2 to 900 W/m^{2,} and the temperature in the drying system was recorded and analyzed. The temperature in the drying system was measured and recorded for 1 h to analyze the effect of using different intensity of artificial solar radiation on the drying. Four 12V DC with 0.55A ventilation fans were used in the solar drying system located at Collector 2, inlet of mixing chamber, outlet of mixing chamber and at the outlet of drying chamber, to control the air velocity and to ensure even distribution of air throughout the system. Besides, fans were used to evacuate humidity released by the products during the drying process. The design detail of the solar drying system is illustrated in Table 3.

Total of twenty-three thermocouples was used in the experiment to record air and absorber temperature. The positioning of the thermocouple in the experimental setup is described further in Table 4, and the location of each thermocouple was presented in Fig. 4 and Fig. 5.
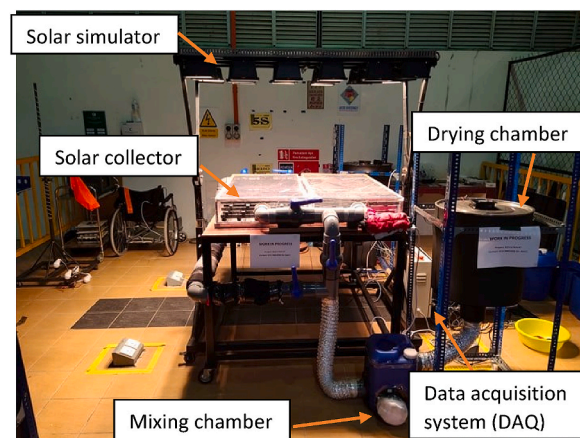

Fig. 3. Setup for a solar drying system.

Table 2

Modes in the solar drying system.

Mode	Heat source
1	Collector
2	Auxiliary Heater
3	Hybrid (Collector + Auxiliary Heater)

Table 3

Design detail of the solar dryer.

Number of collectors	2
Absorber material	Aluminium hollow square tube
Absorber dimension	1.12 m × 0.59 m
Area of aperture	1.219m^2
Working fluid	Air
Insulation material	Insulfex® closed-cell elastomeric nitrile rubber foam
Cover plate material	Polycarbonate
Number of ventilation fan	4
Ventilation fan specifications	12V DC, 0.55A
Drying chamber material	Stainless steel
Drying chamber dimension	0.5 m (diameter), 0.5 (height)

Table 4

Position of thermocouple in the drying system.

Thermocouple	Position
T1	Inlet of solar collector
T2, T3, T4	Absorber Collector 1
T5, T6, T7	Air in Collector 1
T8, T9, T10	Absorber Collector 2
T11, T12, T13	Air in Collector 2
T14	Outlet Collector 1
T15	Outlet Collector 2
T16	Inlet Collector 2
T17	Inlet mixing chamber
T18	Outlet mixing chamber
T19	Inlet drying chamber
T20, T21, T22	Drying chamber
T23	Outlet drying chamber

2.3. Thermal analysis

The thermal power gained in this section was analyzed based on the first law of thermodynamics. The energy rate balance during the experiment was presented in Equation (1):

$$\dot{Q}_A = \dot{Q}_u + \dot{Q}_{loss} \tag{1}$$

where $\dot{Q}_A$, $\dot{Q}_u$ and $\dot{Q}_{loss}$ were the energy absorbed, useful and loss.

The $\dot{Q}_A$ which the power gained by the collector can be express in Equation (2) below:

$$\dot{Q}_A = A_c G \tag{2}$$

The thermal power gain in the system involves the mass flow rate of air, the specific heat capacity of the air and also temperature difference between inlet and outlet of the solar collector. The air passing through each collector undergoes convection with the absorber to produce heat that is transferred into the drying chamber. The energy rate balance can be presented by the following Equation:

$$\dot{Q}_u = \dot{m}_a C_{pa}(T_o - T_i) \tag{3}$$

The mass flow rate was calculated by measuring the velocity of the air across the collector and using the following expression (4):

$$\dot{m}_a = \rho_a A v_a \tag{4}$$

The thermal power gain is proportional to the temperature difference between the inlet and outlet of the collector. The density of air, ρ_a, assumed to be constant at 1.1 kg/m^3, and specific heat capacity of air, C_{pa}, which is 1007 J/kg·K, respectively (Cengel & Boles,
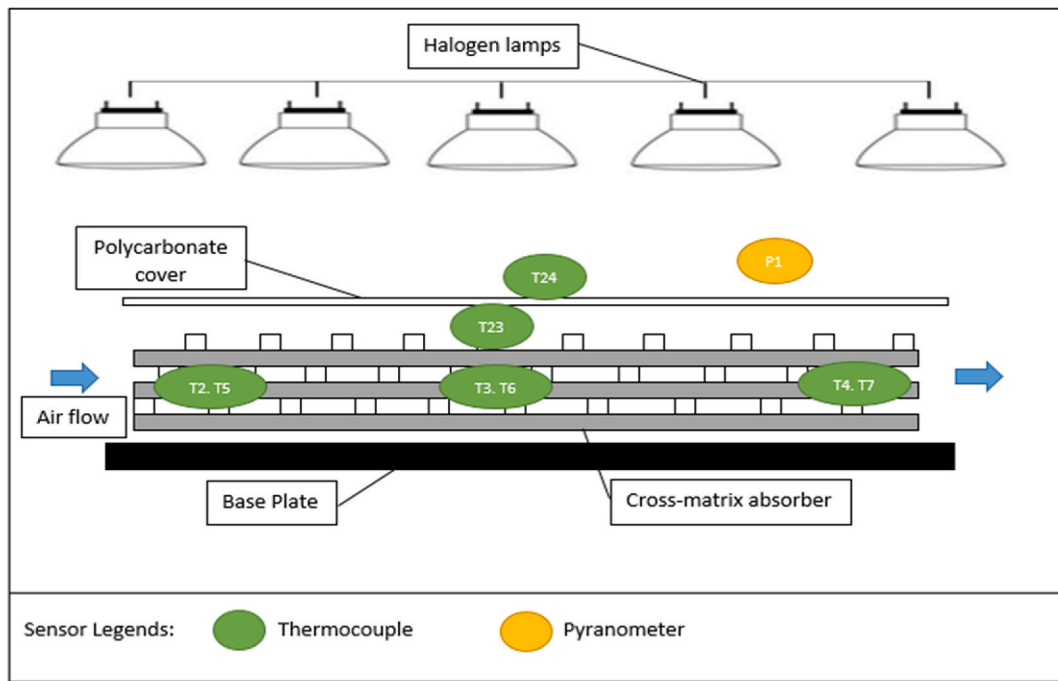
Fig. 4. Schematic diagram for the solar collector with thermocouple location.

2002). Note that Equation (3) is at a low air temperature range between 40 and 60 °C at a pressure of 1 atm.

The thermal energy of the thermal absorber is related to the temperature difference between the initial and final temperature of the cross-matrix absorber, as shown in Equation (5) below:

$$Q_{abs} = m_{abs} \, C_{p,abs} \left(T_{abs, \, initial} - T_{abs, \, final} \right) \tag{5}$$

The fluid flow in the drying system is made possible if the pressure losses are offset by the pumps or fans. The pressure drop in the

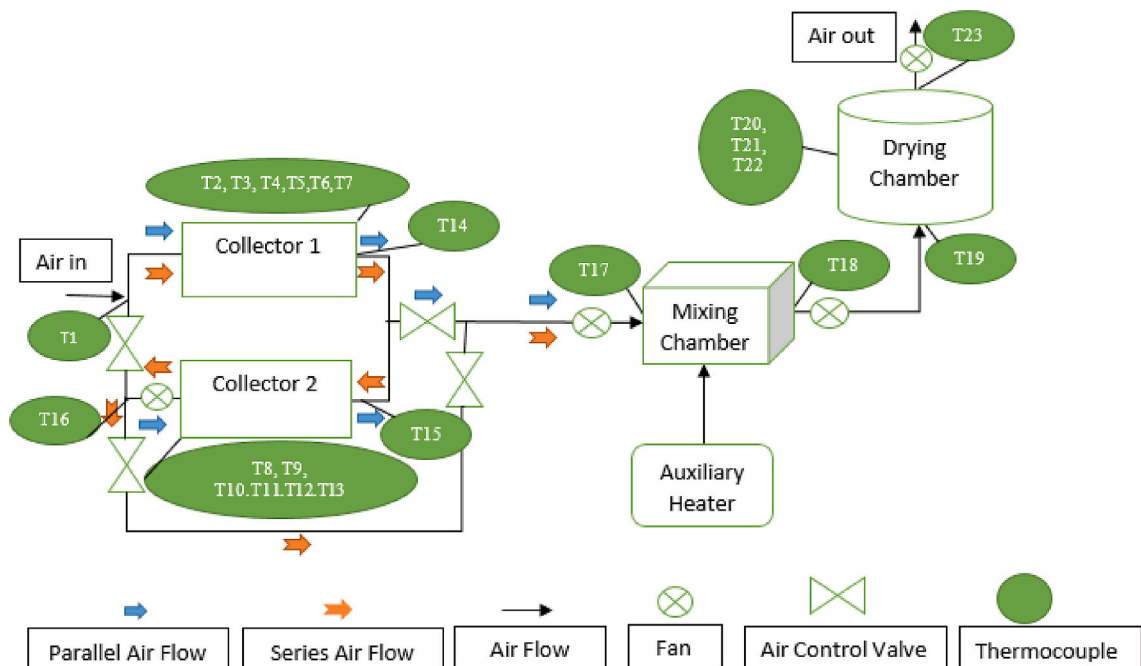**Fig. 5.** Schematic diagram of the solar drying system with thermocouple location.

Table 5

Measuring instruments accuracy.

Instruments	Quantity	Accuracy
K-type thermocouple	23	−1.5 °C to +1.5 °C
Pyranometer	1	0.1 W/m²

Table 6

Parameters uncertainty.

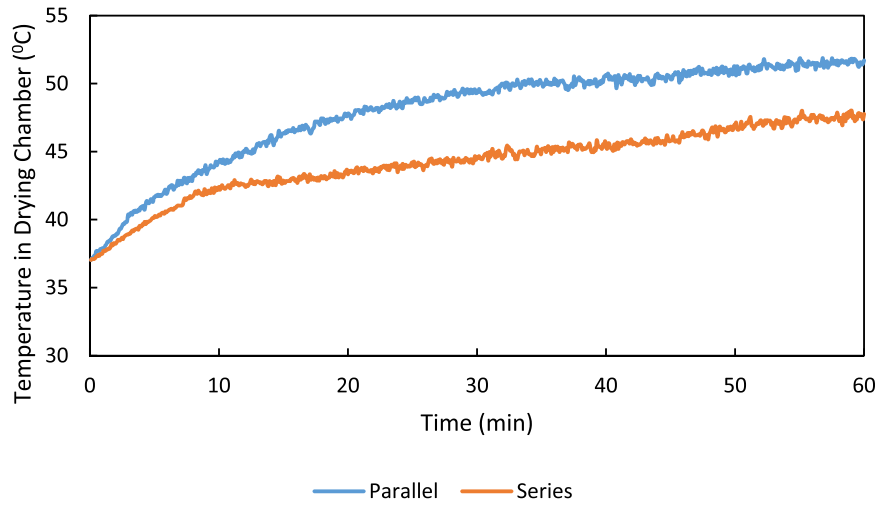| Description	Unit	Uncertainty	Relative uncertainty (%)
Outer temperature	°C	±0.10	0.48
Internal temperature	°C	±0.10	0.72
Ambient temperature	°C	±0.10	0.48
Solar radiation	W/m²	±12	2.04

Fig. 6. Temperature in the drying chamber of series and parallel solar collectors' arrangement.

system was calculated using Bernoulli's principle. The pressure drop between two points, i.e. inlet and outlet, for fluid flow in a pipe is presented by the following Equation (6):

$$P_{fo} - P_{fi} = \frac{1}{2}\rho_f \left(v_{f0}^2 - v_{fi}^2 \right) \tag{6}$$

where P_{fo}, P_{fi}, ρ_f, V_{fo} and V_{fi} are the pressure of the fluid at the outlet (Pa), the pressure of the fluid at the inlet (Pa), the density of heat transfer fluid (kg/m³), the velocity of fluid the outlet (m/s) and velocity at the inlet (m/s), respectively.

The efficiency of each of the component of the system was calculated from the ratio of the output of each component to its input. The efficiency of the collector was determined from the ratio of energy extracted by the heated air through the collector to the total energy gain from the artificial solar radiation by the solar collector. The Equation is written:

$$\eta_c = \frac{\dot{Q}_a}{G\,A_c} = \frac{\dot{V}\rho_a \Delta T C_{pa}}{G\,A_c} \tag{7}$$

The following Equation shows the efficiency of the drying chamber:

$$\eta_d = \frac{Pr\,h_{fg}}{(G\,A_c + W)t} \tag{8}$$

The overall efficiency of the system can be determined by multiplying the efficiencies of each component in the system, as shown below:
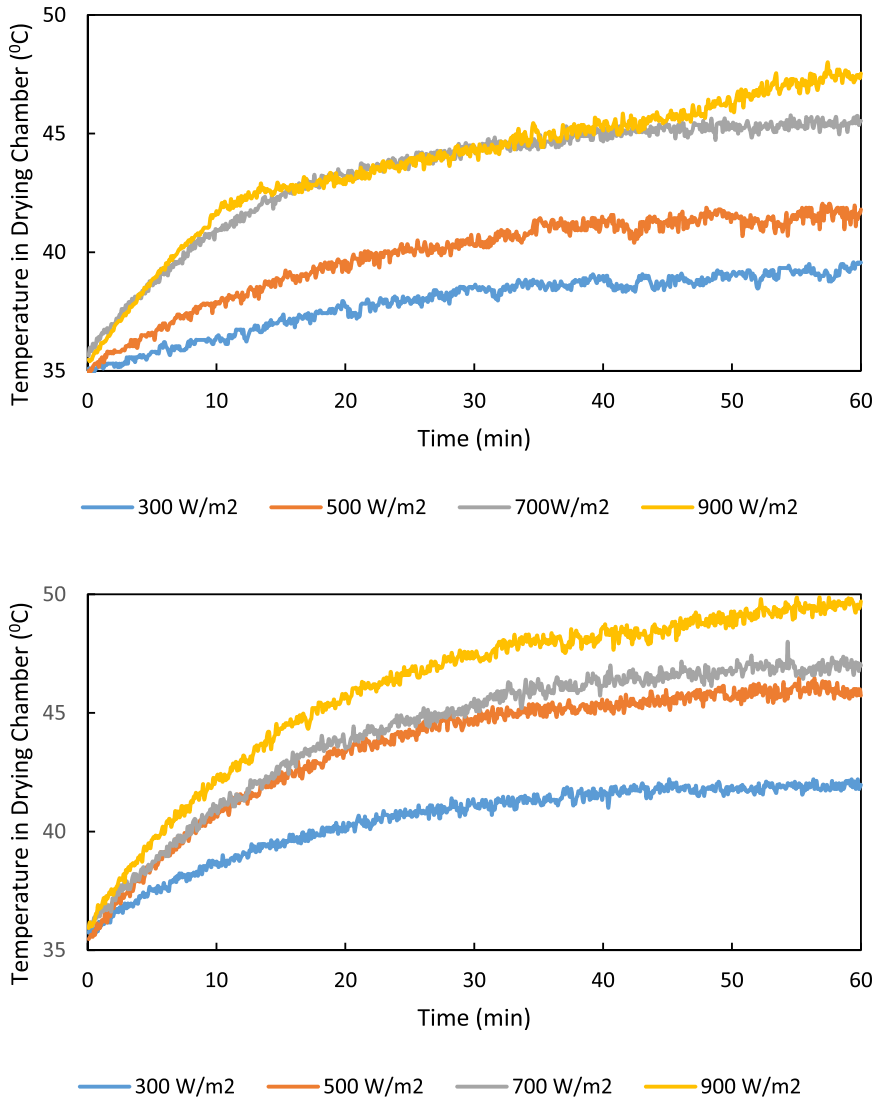
$$\eta_{overall} = \eta_c * \eta_d \tag{9}$$

Fig. 7. aTemperature in the drying chamber for different artificial solar radiation of series collector arrangement.
Fig. 7b: Temperature in the drying chamber for different artificial solar radiation of parallel collector arrangement.

2.4. Uncertainty analysis

The measurements done were subjected to uncertainties, and they were elaborated in this section. The accuracy of each used instrument was determined and presented in Table 5 while the parameters that are studied in this paper involves uncertainty were shown in Table 6 based on the previous study by Refs. [24–26].

Every x_n, number of measurement that had been made have the measurement tolerance of $\sigma_{n,}$ and the uncertainty of the measurement parameters, U_R, can be calculated by using Equation (10) [26]:

$$U_R = \left\{ \left(\frac{U_R}{dx_1}.\sigma_1\right)^2 + \left(\frac{U_R}{dx_2}.\sigma_2\right)^2 + \left(\frac{U_R}{dx_3}.\sigma_3\right)^2 + \ldots \left(\frac{U_R}{dx_n}.\sigma_n\right)^2 \right\}^{\frac{1}{2}} \qquad (10)$$

Based on Equation (10), the uncertainty of the thermal power gained by the system was 257.09 ± 6.29W for series and 314.14 ± 7.68W for parallel with relative uncertainty 2.45% respectively for both modes.
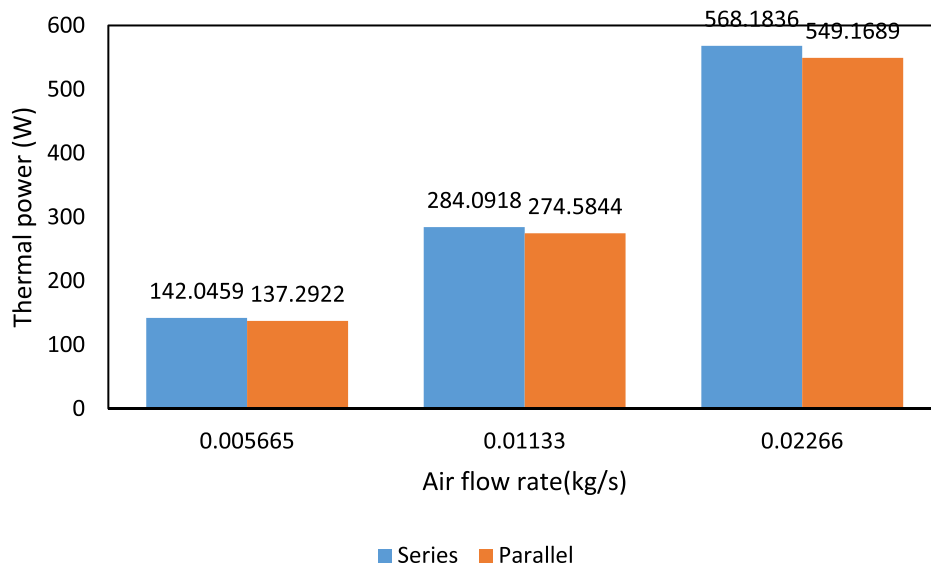
Fig. 8. Thermal power gain for series and parallel configurations at 60 °C.

3. Results and discussion

Fig. 6 presents the variation of drying chamber temperature of series and parallel configurations of a set of cross-matrix solar collectors.

The result shows that parallel configuration of solar collectors for this system is better since it yields higher maximum air temperature inside the drying chamber which is 51.87 °C compared to the series configuration which produces maximum air drying temperature of 48 °C. Even though series configuration produces higher air temperature at the outlet of the solar collectors compared to parallel, higher heat is lost to the surrounding due to the extended air pathway entering the drying chamber.

For series solar collector arrangement, the airflow at the inlet of the second collector corresponds to the airflow of the outlet of the first collector. Higher output air temperature is produced by series configuration compared to parallel since the airflow is divided at the entrance of each of solar collectors for parallel configuration, making the air outlet temperature similar [27]. The air temperature flowing from the collectors to the drying chamber corresponds to the air temperature at the outlet of the solar collectors.

However, higher air temperature produced by the collectors leads to higher thermal losses. Especially for the collectors in a series arrangement, the heated air needs to travel a longer path, thus causing more friction losses. The moving air particles tend to collide with the ducting surface, causing heat conduction at the impact area [28]. Hence, the thermal energy and air temperature decrease as it travels along with the ducting until it enters the drying chamber. In contrast, a parallel arrangement solar collector is more efficient compared to series due to shorter air path and lesser collision between the air and pipe surface, which leads to lower thermal losses and resulting in higher air temperature inside the drying chamber.

In a drying process, the temperature is an essential parameter where it influences the drying rate and the final product's quality. By providing higher air temperature inside a drying chamber, the drying process can be shortened due to high drying rate, when the initial moisture content inside the product is high.

The effect of variations of artificial solar radiation on the air temperature in the drying chamber for this solar drying system for both series and parallel collectors' arrangement is shown in Fig. 7a and Fig. 7b. The experiment was conducted indoor with ambient temperature varying from 30 °C to 33 °C. The solar simulator used in the experiment to represent solar radiation was set to range between 300W/m^2 to 900W/m^2. As expected, after 1 h, it was observed artificial solar radiation of 900W/m^2 produced highest heated air temperature in the drying chamber for both series and parallel collector configurations, namely 47.53 °C and 49.87 °C. Meanwhile, other artificial solar radiation values like 300W/m^2, 500W/m^2 and 700 W/m^2 produced lower air temperature inside drying chamber, namely 39.57 °C, 41.80 °C and 45.53 °C for series and 41.97 °C, 45.73 °C and 47.07 °C for parallel configurations. It is due to more radiation converted into heat energy that causes the molecules of the absorber to vibrate. The vibration increases the temperature of the material as the temperature is proportional to the kinetic energy [29]. The heat is extracted by the air that passes through the absorber due to better heat removal factor possessed by square tube thermal absorbers. Higher radiation will produce more considerable heat energy into the drying chamber and hence accelerate the drying process. In a solar drying system, the intensity of solar radiation is essential since it determines the efficiency of the system [30].

From this experiment, for both series and parallel configurations, it can be analyzed that maximum temperature inside the drying chamber can be reached after 50 min of exposure to artificial solar radiation. After this period, the temperature in the drying chamber is maintained until the end of the experiment. This shows that the air in the drying chamber has reached the terminal temperature of equilibrium of the drying air.

Total thermal power gain is obtained by relating the mass flow rate with specific heat capacity and the temperature difference
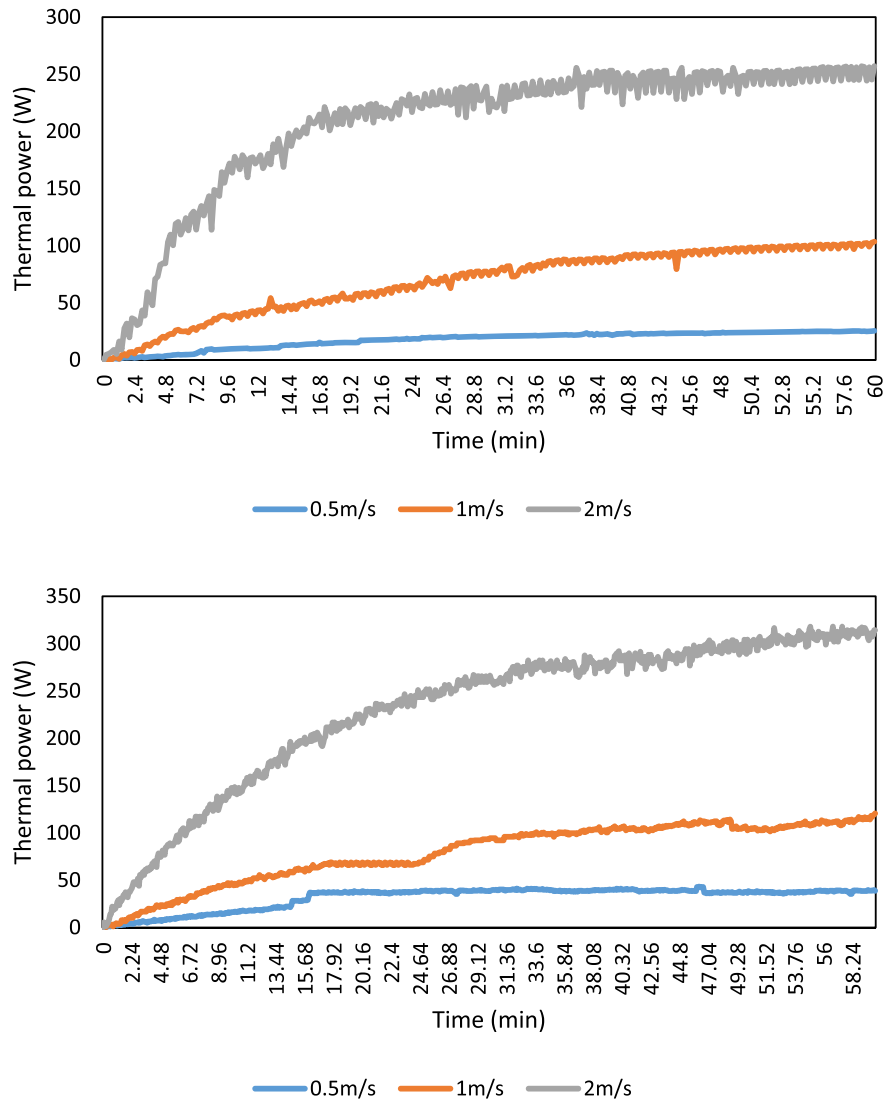
Fig. 9. aThermal power gained in 1 h (series configuration).
Fig. 9bThermal power gain in 1 h (parallel configuration).

between the beginning and end of the experiment. From Fig. 8, it is observed that the mass flow rate at a constant drying chamber temperature of 60 °C influences the power gain in the system. Higher air mass flow rate leads to higher power gain in the drying chamber due to the increment of heat removal factor at the solar air collector section. Higher air mass flow rate achieved using higher air velocity will increase the heat transfer coefficient between the moving air and the thermal absorber, which enhanced the heat transfer rate between the two. This event subsequently increases the air temperature in the drying chamber, triggering the air molecule to increase their average speed and resulting in more substantial kinetic energy. Hence, the increase in airflow rate has an essential and favorable effect on the overall energetic performance of the solar collectors [31].

Fig. 9a–b shows the thermal power gain in the drying chamber after 1 h for series solar collector arrangement. The power achieved for series arrangement was 25.48W, 103.44W and 257.09W for air velocity of 0.5 m/s, 1 m/s and 2 m/s, respectively. Meanwhile, the power gain for parallel arrangement after 1 h was 38.79W, 120.59W and 314.14W, respectively. It is since higher air velocity increases the heat removal factor for the flowing air across the thermal absorber. By comparing the two collector arrangements, it can be seen that the parallel collector arrangement produces more power than the series arrangement. The average temperatures in the drying chamber for series and parallel collector arrangements are 48 °C and 49.87 °C, respectively. Even though the temperature difference is just 1.87 °C, there is a significant difference in the power gain, which is 57.09W. In terms of power gain, it is, therefore, preferable to use the parallel collector arrangement since it provides a shorter airflow path, simultaneously reducing more heat losses to the sur- rounding. The power losses from the system are shown in Fig. 10, where the series collector arrangement with 0.5 m/s air velocity
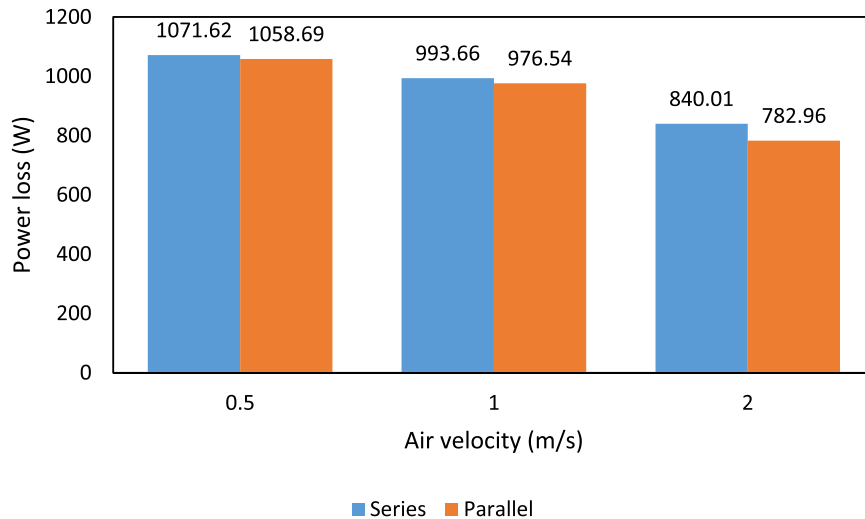
Fig. 10. Power loss for series and parallel configuration.

Table 7
Pressure drop points description.

Point	Region
1	Inlet collector – Surrounding
2	Outlet collector – Inlet Collector
3	Inlet mixing chamber – Outlet collector
4	Outlet mixing chamber – Inlet mixing chamber
5	Inlet Drying Chamber – Outlet mixing chamber
6	Outlet Drying Chamber – Inlet Drying Chamber

experienced the highest losses compared to parallel modes and higher air velocity.

The pressure differential between two points is essential to keep the fluid flowing in a system. It will be produced when fluid is flowing through ducts with obstacles that result in resistance for the fluid to flow. In this solar dryer system, the resistance occurs at the collector inlet-outlet, pipe joints, change in elevation of the fluid and also due to ventilation fans. Different pressure drop regions are presented in Table 7.

Fig. 11a and Fig. 11b present the recorded total pressure drop values at inlet and outlet of each component of the drying system for both series and parallel solar collectors arrangement. From the obtained results, it is observed that the pressure drop throughout each component in the system fluctuates according to resistances and usage of ventilation fans that control the airflow. Higher air velocity results in a significant pressure drop following Equation (4) where pressure drop is proportional to the difference between the squared value of the outlet and inlet fluid velocity of each component. The pressure drop at air velocity of 2 m/s for series and parallel collector arrangement at Point 5 are 1.4 kPa and 3.6 kPa, while for 1 m/s are 0.35 kPa and 0.9 kPa, and for 0.5 m/s are 0.088 kPa and 0.23 kPa.

It is also observed that fluid temperature influences the value of the total pressure drop. This relation can be analyzed by comparing Point 2 in the graph for series and parallel collector arrangements with constant air velocity. For air velocity of 0.5 m/s, 1 m/s and 2 m/s, the pressure drop values for series arrangement are -0.08 kPa, -0.33 kPa and -1.3 kPa. The negative values indicate the air flowing from high to low-pressure regions. Meanwhile, for the parallel arrangement, the pressure drop values are 0.1 kPa, 0.4 kPa and 1.6 kPa. From the result, it is shown that the values of total pressure drop for series collector arrangement are lower than the parallel arrangement. This is due to higher air temperature produced at the outlet for series arrangement compared to parallel. The increase of fluid temperature will lead to a decrease in the fluid density, which will cause declination to the total pressure drop value.

The use of ventilator fan is essential, especially in solar drying system to provide the required airflow, reduce the drying time and as well act as a fluid flow booster to reduce friction flow in the system. The ventilator function is to assist the airflow from the solar collector into the drying chamber. It can reduce potential heat losses carried by air during the heat transportation to the drying chamber. It increases the air pressure to keep the airflow from higher to a lower air pressure area.

It can be observed that between Points 2 and 3 as well as between Points 4 and 5 in both configurations, there is a sudden increased in pressure drop. In parallel collector arrangement, at an air velocity of 2 m/s, the pressure drop value increase from 1.6 kPa to 2.8 kPa from point 2 to 3, and there is also a sudden increase of pressure drop values from -6kPa to 3.6 kPa from point 4 to 5, but at 0.5 m/s of air velocity, the pressure drop value increase from 0.1 kPa to 0.18 kPa from point 2 to 3, and there is also a sudden increase of pressure drop values from -0.38 kPa to 0.23 kPa from point 4 to 5.
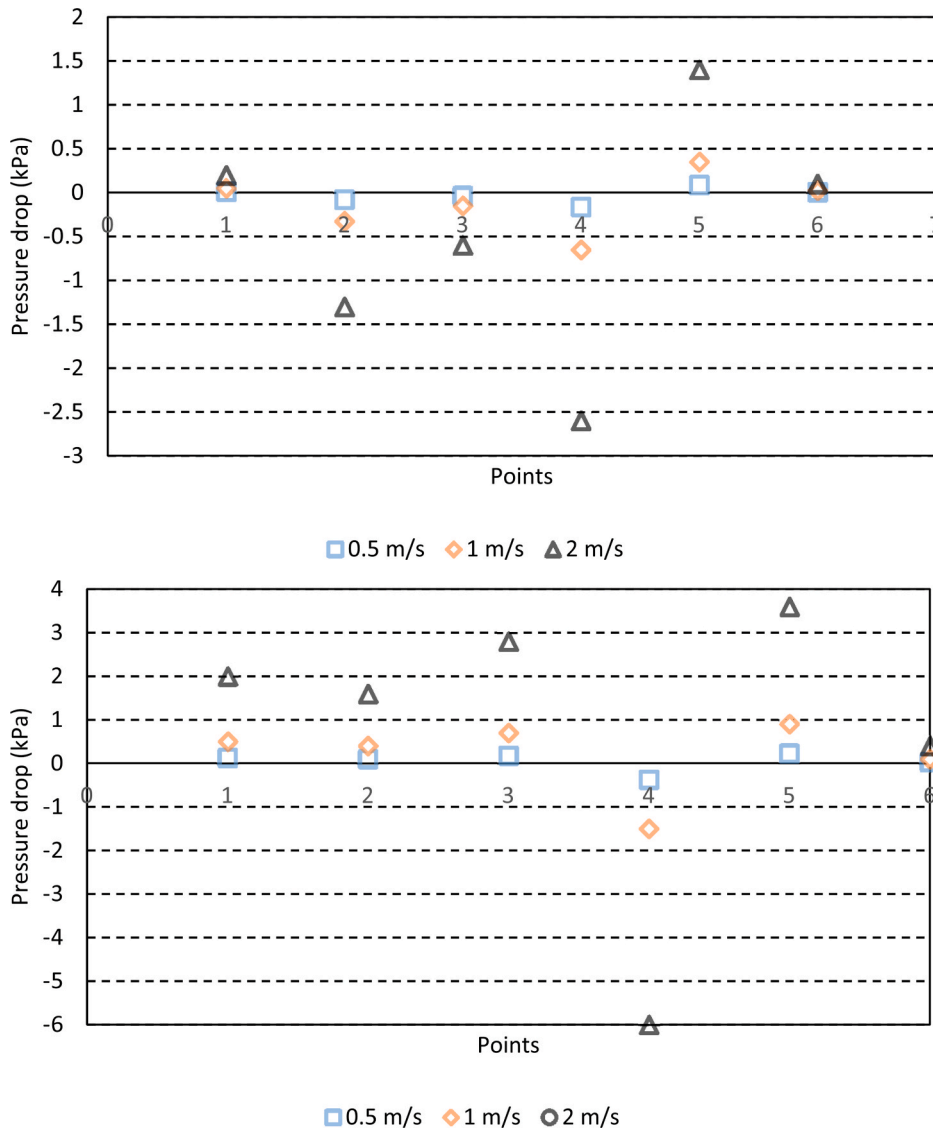
☐ 0.5 m/s　◇ 1 m/s　△ 2 m/s

☐ 0.5 m/s　◇ 1 m/s　⬡ 2 m/s

Fig. 11. aPressure drop in solar drying system of series collector arrangement.
Fig. 11bPressure drop in solar drying system of parallel collector arrangement.

Table 8
Pressure drop values at each point.

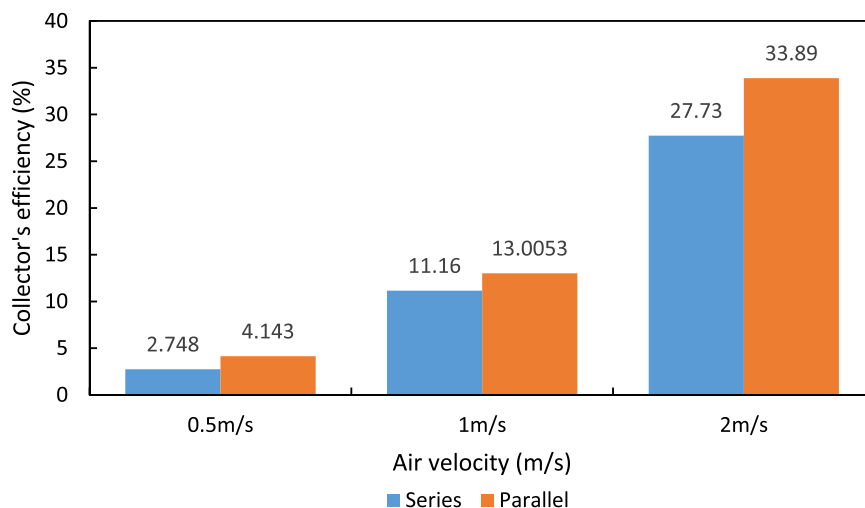| Pressure drop point (kPa)	V= 0.5 m/s			V= 1 m/s			V= 2 m/s		
	ΔP_{series}	$\Delta P_{parallel}$	$|\Delta P_{series-parallel}|$	ΔP_{series}	$\Delta P_{parallel}$	$|\Delta P_{series-parallel}|$	ΔP_{series}	$\Delta P_{parallel}$	$|\Delta P_{series-parallel}|$
1	0.01	0.13	0.11	0.05	0.50	0.45	0.20	2.00	1.80
2	−0.08	0.10	0.18	−0.33	0.40	0.08	−1.30	1.60	2.90
3	−0.04	0.18	0.21	−0.15	0.70	0.85	−0.60	2.80	3.40
4	−0.16	−0.38	0.21	−0.65	−1.50	0.85	−2.60	−6.00	3.40
5	0.09	0.23	0.14	0.35	0.90	0.55	1.40	3.60	2.20
6	0.01	0.03	0.02	0.03	0.10	0.08	0.10	0.40	0.30

Fig. 12. Comparison of collectors' efficiency between series and parallel collector's arrangement.

This increase implies the higher the velocity of air across the system; the higher will be the mass flow rate, and consequently, the pressure drop will also increase [13]. At Point 3, there was a ventilation fan placed at the inlet of the mixing chamber. The fan provided suction condition to accelerate the heat transferring process from the collector to the mixing chamber. At Point 4, the pressure drop value decreases drastically, due to the design of the mixing chamber itself. This is because of the outlet channel above the inlet channel of the mixing chamber causing higher air pressure required to push the air. A ventilation fan was installed at the outlet of the mixing chamber to create negative pressure leading to low-pressure losses in the system. The negative pressure created will allow the air to flow to a lower pressure different region [16].

From Table 8, lower pressure drops are recorded for series collector arrangement compared to parallel; lower differential signifies a lower power consumption and vice versa. Despite the favorable of a low-pressure drop in solar dryer application, however, it does not have a significant impact for this solar dryer. The ventilation fans helped the system to increase the air velocity, which reduced potential heat losses that result in more heat can be transferred into the drying chamber. Besides, design for parallel collector arrangement that shortens the air path can ensure higher efficiency compared to series arrangement even though the pressure drop values are higher. Hence, the pressure drop issue causes a smaller impact on this solar dryer performance.

Fig. 12 presents the results of the efficiency of the collector, which varies with solar collectors' arrangement and the air velocity. The efficiency of parallel arrangement is higher compared to series, namely 4.14%, 13% and 33.98% at an air velocity of 0.5 m/s, 1 m/s and 2 m/s, respectively. Meanwhile, the efficiency for the series collector is 2.75%, 11.16% and 27.73% at similar air velocities. This is related to parallel arrangement producing a higher ratio of output energy to total heat that had been taken in compared to the series collector arrangement. There is also a significant difference between the efficiencies achieved with that of different air velocities. Higher air velocity produces higher efficiency since lesser heat is lost to the surrounding during the test, leading to higher energy gain in the drying chamber.

Two drying tests of kaffir lime leaves were conducted using series and parallel collector arrangements. The drying process parameters were set at 900W/m^2 of artificial solar radiation and air velocity of 2.0 m/s. A total of 40g of kaffir lime leaves was placed on four layers of trays, and they were dried until they reached their equilibrium mass of 16 g.

Fig. 13a and b shows the results of the drying activities. It can be deduced that the drying period using parallel collector arrangement can be reduced by about 17.65% compared to series collector arrangement since the time taken for parallel collector arrangement was 7.0 h. In contrast, for the series arrangement, the time taken was 8.5 h. It is due to different heated air temperature achieved inside the drying chamber when using both arrangements. The average air temperature for the parallel arrangement was 49.98 °C, while for the series arrangement, it was 47.02 °C. The trend shows that drying time is inversely proportional to air temperature. With the increase in air temperature, the time required to reduce the kaffir lime leaves mass decreases. Higher air temperature can lead to higher energy availability to remove moisture from the kaffir lime leaves, hence resulting in a higher drying rate for the process. The efficiency of the drying system using parallel configuration is 31.82%. In contrast, lower efficiency is produced by series configuration, which is 22.41%, as shown in Fig. 14. From the presented results, it can be seen that the increase of solar dryer thermal performance resulting from the higher thermal gain by the parallel solar collector arrangement than the series configuration.
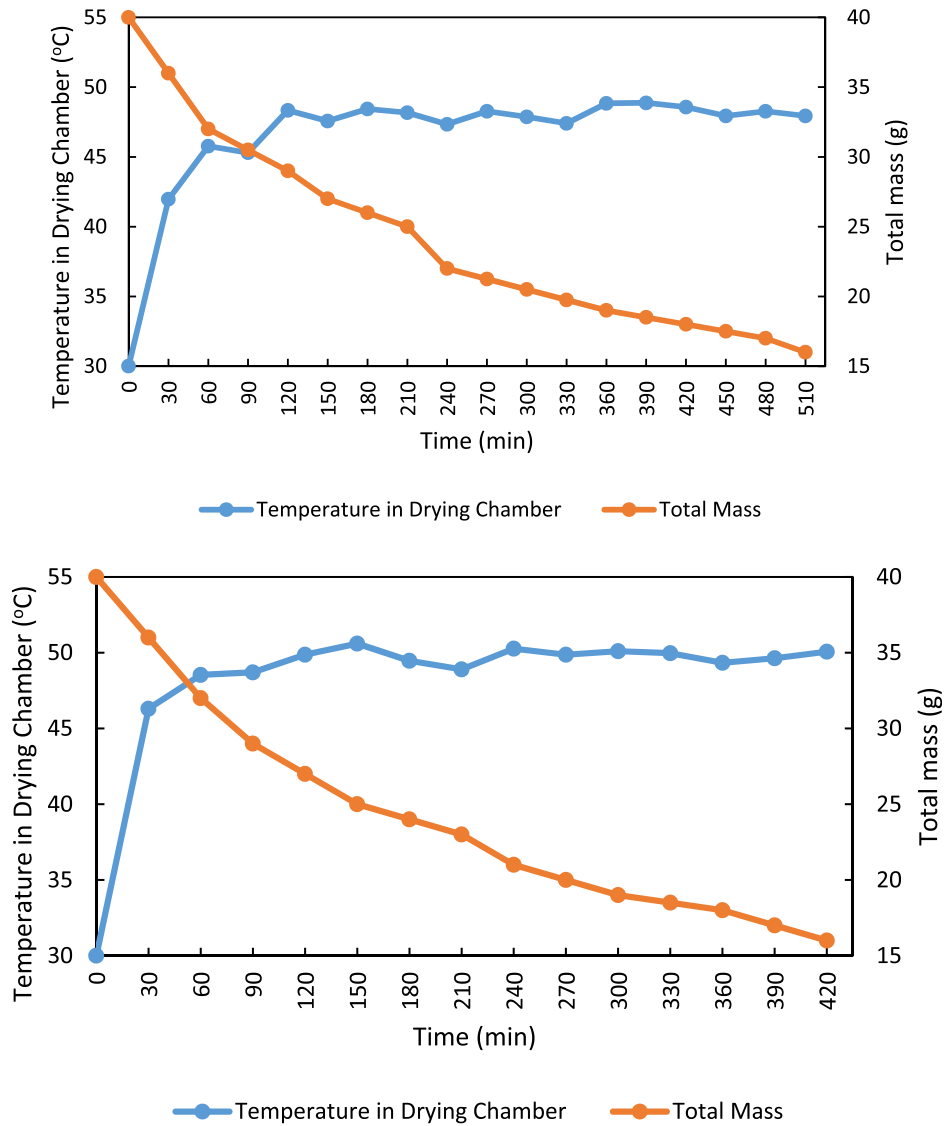
Fig. 13. aDrying of kaffir lime leaves using series configuration.
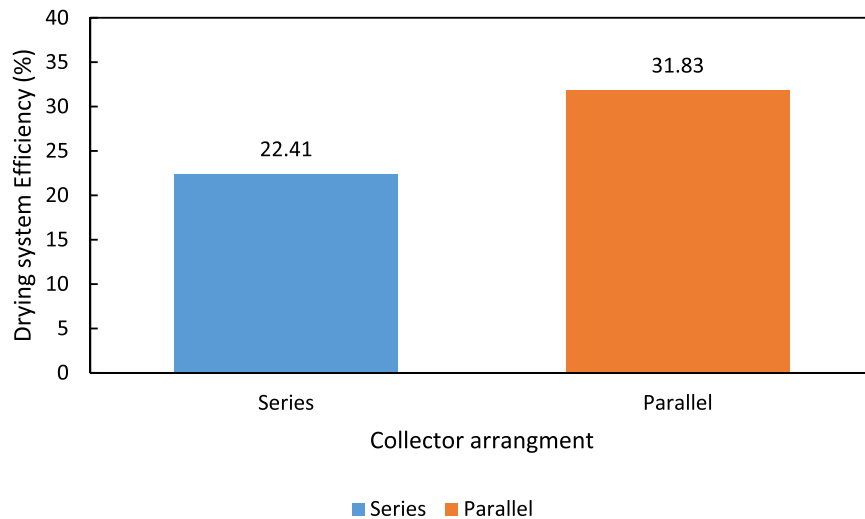Fig. 13bDrying of kaffir lime leaves using parallel configuration.

Fig. 14. Drying system efficiency of the solar dryer for series and parallel collector arrangement.

4. Conclusion

The arrangement of solar collectors either in series or in parallel affects the performance of a solar drying system. Parallel collector arrangement has higher efficiency than the series regarding the air temperature value in the drying chamber, energy consumption, and thermal efficiency due to the shorter air path between the collector and drying chamber. The maximum air temperature achieved inside the drying chamber for the parallel arrangement was 4 °C higher than the series arrangement when the air velocity was increased to 2 m/s. Parallel collector arrangement leads to higher pressure drop values rather than series. The values are proportional to the square value of the difference between air velocity at the outlet and inlet of each component. The use of ventilation fans created higher air pressure to allow airflow to a lower air pressure region. There was a difference of 3.38 kJ of thermal energy gain using 2 m/s of air velocity between collector arrangements, namely 18.59 kJ for parallel and 15.21 kJ for series configuration, which leads to a drying efficiency of 33.89% for parallel compared to 27.72% for series configurations.

CRediT authorship contribution statement

M.A.S.M. Tarminzi: Data curation, Investigation, Writing – original draft, Investigation. **A.A. Razak:** Supervision, Conceptualization, Methodology. **M.A.A. Azmi:** Investigation, Validation. **A. Fazlizan:** Validation, Methodology, Project administration, Writing – review & editing. **Z.A.A. Majid:** Resources. **K. Sopian:** Funding acquisition, Writing – review & editing.

Declaration of competing interest

The authors declare that they have no known competing financial interests or personal relationships that could have appeared to influence the work reported in this paper.

Nomenclature

A	area (m^2)
C_p	specific heat capacity (kJ/kg K)
G	solar irradiance (W/m^2)
h_{fg}	latent heat of evaporation (J/kg)
$\dot{m}$	mass flow rate (kg/s)
P	pressure (Pa)

Pr	productivity of the system (kg)
Q	thermal power gain (W)
T	temperature (^{0}C)
t	time (s)
U_R	uncertainty
V	volume flow rate (m^3/s)
v	velocity (m/s)
W	auxiliary heater power (W)
ρ	density (kg/m^3)
η	efficiency
ΔT	temperature difference (^{0}C)
σ	tolerance

Subscript

a	air
c	collector
d	drying chamber
f	fluid
o	outlet
i	inlet

References

[1] E. Sivakumar, K. Rajesh, Different types of solar dryer for agricultural and marine products: a reference guide, Int. J. Res. Sci. Technol. III (2016) 118–125, https://doi.org/10.1029/2001GB001639.

[2] M. Absi Halabi, A. Al-Qattan, A. Al-Otaibi, Application of solar energy in the oil industry - current status and future prospects, Renew. Sustain. Energy Rev. (2015), https://doi.org/10.1016/j.rser.2014.11.030.

[3] A.G. Olabi, Circular economy and renewable energy, Energy (2019), https://doi.org/10.1016/j.energy.2019.05.196.

[4] S.H. Farjana, N. Huda, M.A.P. Mahmud, R. Saidur, Solar process heat in industrial systems – a global review, Renew. Sustain. Energy Rev. (2018), https://doi.org/10.1016/j.rser.2017.08.065.

[5] P. Tzoumanikas, E. Nikitidou, A.F. Bais, A. Kazantzidis, The effect of clouds on surface solar irradiance, based on data from an all-sky imaging system, Renew. Energy 95 (2016) 314–322, https://doi.org/10.1016/j.renene.2016.04.026.

[6] H. El, A. Herez, M. Ramadan, H. Bazzi, M. Khaled, An investigation on solar drying : a review with economic and environmental assessment, Energy 157 (2018) 815–829, https://doi.org/10.1016/j.energy.2018.05.197.

[7] M.E.A. Slimani, M. Amirat, S. Bahria, I. Kurucz, M. Aouli, R. Sellami, Study and modeling of energy performance of a hybrid photovoltaic/thermal solar collector: configuration suitable for an indirect solar dryer, Energy Convers. Manag. 125 (2016) 209–221, https://doi.org/10.1016/j.enconman.2016.03.059.

[8] M.E.A. Slimani, R. Sellami, A. Mahrane, M. Amirat, Study of hybrid photovoltaic/thermal collector provided with finned metal plates: a numerical investigation under real operating conditions, in: *2019* International Conference on Advanced Electrical Engineering, ICAEE 2019, (March 2020), 4–5, 2019, https://doi.org/10.1109/ICAEE47123.2019.9015175.

[9] A. Fudholi, K. Sopian, M.H. Ruslan, M.A. Alghoul, M.Y. Sulaiman, Review of solar dryers for agricultural and marine products, Renew. Sustain. Energy Rev. 14 (1) (2010) 1–30, https://doi.org/10.1016/j.rser.2009.07.032.

[10] S. Ratner, K. Gomonov, S. Revinova, I. Lazanyuk, Energy saving potential of industrial solar collectors in southern regions of Russia: the case of krasnodar region, Energies 13 (4) (2020), https://doi.org/10.3390/en13040885.

[11] G. Colangelo, E. Favale, P. Miglietta, A. De Risi, Innovation in flat solar thermal collectors: a review of the last ten years experimental results, Renew. Sustain. Energy Rev. (2016), https://doi.org/10.1016/j.rser.2015.12.142.

[12] Z.A.A. Majid, A.A. Razak, M.H. Ruslan, K. Sopian, Characteristics of solar thermal absorber materials for cross absorber design in solar air collector, Int. J. Automot. Mech. Eng. 11 (1) (2015) 2582–2590, https://doi.org/10.15282/ijame.11.2015.36.0217.

[13] A.A. Razak, Z.A.A. Majid, F. Basrawi, A.F. Sharol, M.H. Ruslan, K. Sopian, A performance and technoeconomic study of different geometrical designs of compact single-pass cross-matrix solar air collector with square-tube absorbers, Sol. Energy 178 (December 2018) (2019) 314–330, https://doi.org/10.1016/j.solener.2018.12.010.

[14] A.F. Sharol, A.A. Razak, Z.A.A. Majid, M.A.A. Azmi, M.A.S.M. Tarminzi, Performance of force circulation cross-matrix absorber solar heater integrated with latent heat energy storage material, IOP Conf. Ser. Mater. Sci. Eng. 469 (1) (2019), https://doi.org/10.1088/1757-899X/469/1/012107.

[15] W. Braham, A. Khellaf, A. Mediani, M. El, A. Slimani, A. Loumani, A. Hamid, Experimental investigation of an active direct and indirect solar dryer with sensible heat storage for camel meat drying in Saharan environment, Sol. Energy 174 (April) (2018) 328–341, https://doi.org/10.1016/j.solener.2018.09.037.

[16] A.A. Razak, Performance of Bi-metallic Cross Matrix Absorber in Air Based Solar Air Collector, PhD Thesis, 2017. Universiti Kebangsaan Malaysia.

[17] M. Koussa, D. Saheb, H. Belkhamsa, M.A. Lalaoui, S.A. Hakem, S. Sami, H. Mustapha, Effect of parallel and serie connection configuration of solar collector on the solar system performances, in: 2015 6th International Renewable Energy Congress, IREC 2015, (December 2016), 2015, https://doi.org/10.1109/IREC.2015.7110957.

[18] M. Ricci, E. Bocci, E. Michelangeli, A. Micangeli, M. Villarini, V. Naso, Experimental tests of solar collectors prototypes systems, Energy Procedia 82 (2015) 744–751, https://doi.org/10.1016/j.egypro.2015.11.804.

[19] A. Kotb, M.B. Elsheniti, O.A. Elsamni, Optimum number and arrangement of evacuated-tube solar collectors under various operating conditions, Energy Convers. Manag. 199 (May) (2019), 112032, https://doi.org/10.1016/j.enconman.2019.112032.

[20] E. Vengadesan, R. Senthil, A review on recent development of thermal performance enhancement methods of flat plate solar water heater, Sol. Energy 206 (June) (2020) 935–961, https://doi.org/10.1016/j.solener.2020.06.059.

[21] P. Rhushi Prasad, H.V. Byregowda, P.B. Gangavati, Experiment analysis of flat plate collector and comparison of performance with tracking collector, Eur. J. Sci. Res. 40 (1) (2010).

[22] A.M. Shariah, A. Rousan, K.K. Rousan, A.A. Ahmad, Effect of thermal conductivity of absorber plate on the performance of a solar water heater, Appl. Therm. Eng. (1999), https://doi.org/10.1016/S1359-4311(98)00086-6.

[23] G. Alvarez, J. Arce, L. Lira, M.R. Heras, Thermal Performance of an Air Solar Collector with an Absorber Plate Made of Recyclable Aluminum Cans, vol. 77, 2004, pp. 107–113, https://doi.org/10.1016/j.solener.2004.02.007.

[24] R.J. Moffat, Contributions to the theory of single-sample uncertainty analysis, J. Fluids Eng. Trans. ASME 104 (2) (1982) 250–258, https://doi.org/10.1115/1.3241818.

[25] M. Yahya, A. Fudholi, K. Sopian, Energy and exergy analyses of solar-assisted fluidized bed drying integrated with biomass furnace, Renew. Energy 105 (2017) 22–29, https://doi.org/10.1016/j.renene.2016.12.049.

[26] Sharol, Fadzil Ahmad, A. Abdul Razak, Z.A. Abdul Majid, A. Fudholi, Experimental study on performance of square tube absorber with phase change material, Int. J. Energy Res. 44 (2) (2020) 1000–1011, https://doi.org/10.1002/er.4971.

[27] J.M. Jalil, K. Faisal, L. Rasheed, S. Marcos, Numerical and Experimental Investigation of Solar Air Collectors Performance Numerical and Experimental Investigation of Solar Air Collectors Performance Connected in Series, 2017 (January).

[28] J. Sun, M.M. Chen, A theoretical analysis of heat transfer due to particle impact, Int. J. Heat Mass Tran. 31 (5) (1988) 969–975, https://doi.org/10.1016/0017-9310(88)90085-3.

[29] Walker Jearl, Fundamentals of Physics Halliday & Resnick 10ed, Wiley, 2007.

[30] F. Sulaiman, N. Abdullah, Z. Aliasak, Solar drying system for drying empty fruit, Bunches 24 (1) (2013) 75–93.

[31] M. El, A. Slimani, M. Amirat, S. Bahria, I. Kurucz, M. Aouli, Study and modeling of energy performance of a hybrid photovoltaic/thermal solar collector : configuration suitable for an indirect solar dryer, Energy Convers. Manag. 125 (2016) 209–221, https://doi.org/10.1016/j.enconman.2016.03.059.